Molecular-dynamics studies of grain-boundary diffusion. II. Vacancy migration, diffusion mechanism, and kinetics

Thomas Kwok and Paul S. Ho
IBM Thomas J. Watson Research Center, Yorktown Heights, New York 10598

Sidney Yip
Department of Nuclear Engineering, Massachusetts Institute of Technology, Cambridge, Massachusetts 02139
(Received 22 December 1983)

Vacancy jumps in a bicrystal model of $\Sigma=5$ (36.9°) [001] tilt boundary in bcc Fe have been simulated at temperatures of 1300, 1400, and 1500 K by molecular dynamics with the use of the empirical Johnson potential. The results confirm the dominance of a vacancy mechanism in grain-boundary diffusion. An activation energy of 0.51 eV for vacancy migration has been obtained along with a reasonable value of the jump-attempt frequency. Analysis of the jump directions shows a preferential bias along the tilt axis. The relation between diffusivity and atomic mean-square displacement is examined. It is suggested that the structure dependence of grain-boundary diffusion may be expressed through a matrix of transition probability for vacancy jumps among the various discrete sites.

I. INTRODUCTION

Grain-boundary (GB) diffusion is a basic process governing the kinetics of microstructural change during metallurgical processes and applications.[1] Its importance lies in the fact that diffusion in metals occurs more rapidly along GB's than through the lattice. Recent attempts to understand this phenomenon have focused on the mechanism of diffusion.[1,2] While measurements on activation volume for diffusion[3] and on the isotope effect[4] in the case of Ag suggests that the vacancy mechanism dominates in GB diffusion, it would be of considerable interest to demonstrate this explicitly by directly observing the details of the vacancy motion and relating the dynamical events to the observed diffusivity. Such an approach may not be practiceable in laboratory experiments, but it is quite feasible with computer molecular-dynamics (MD) simulation.

In the preceding paper[5] (hereafter referred to as I) we have reported a simulation study of the structural properties and defect mobility in a $\Sigma=5$ (36.9°) [001] tilt boundary in bcc Fe using the empirical Johnson potential. Here we will describe the analysis of vacancy migration and diffusion kinetics. Our results, based in the several hundred vacancy jumps observed at each of three temperatures, give very reasonable values for the activation energy for vacancy migration, the attempt frequency for vacancy jump, and the anisotropy of jumps parallel and perpendicular to the tilt axis, thus providing molecular evidence for the vacancy mechanism of diffusion.[6,7]

To relate the vacancy jumps to diffusivity, one needs to calculate an appropriate correlation factor. We choose the alternative of extracting the diffusivity from the atomic mean-square displacement function in the same manner as we would proceed in analyzing diffusion in liquids. Our attempt thus far is only partly successful because of two limiting factors. The first is the practical difficulty of accumulating sufficient data on atomic jumps rather than vacancy jumps. The second is the inherent ambiguity of defining the boundary width and therefore those atoms to be considered in calculating the mean-square displacement function.

II. OBSERVATION OF VACANCY JUMPS

All the simulation runs reported here were carried out with the initial configuration being the relaxed GB structure at $T=0$ K with a vacancy inserted at site B in the middle of the simulation system (atomic layer 5 in Fig. 1 of I). The system was then brought up to the desired temperature and allowed to equilibrate. During the simulation the system volume was not allowed to change; however, at several temperatures the system dimension was adjusted for thermal-expansion effects so as to maintain more or less the same pressure at different temperatures of simulation. Each run corresponds to sampling a (N,V,E) ensemble, where E is the total energy, kinetic plus potential.

We performed long simulation runs at three temperatures, 1300, 1400, and 1500 K. Table I shows the number of vacancy jumps observed in each case. The jump rates were obtained by dividing the number of jumps by the simulation time, which was 390 psec based on a reduced time-step size of $t=0.3324\times10^{-14}$ sec. Notice that these rates refer to the total number of vacancy jumps in the system irrespective of the number of vacancies in the system. At $T=1300$ K there was only one vacancy during most of the simulation period, but at $T=1500$ K the probability of having multiple vacancies at any time has increased significantly. The entry in Table I merely indicates that the number of vacancy jumps at $T=1500$ K was the result of counting four distinct vacancy trajectories. Table I also shows several shorter runs. Their statistics are such that the results have, at best, only quali-

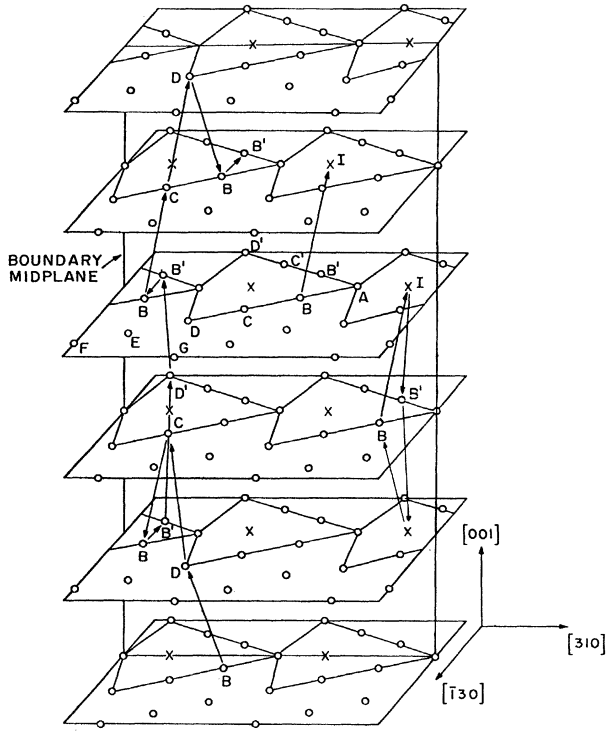

FIG. 1. A portion of vacancy trajectory observed during simulation at $T=1500$ K. Length scale along [001] has been magnified by a factor of 5.

tative significance. Still, these data provide additional information concerning the behavior at higher temperatures. Beyond 1500 K, data analysis for discrete vacancy jumps become very difficult because the vacancies were no longer well localized and at the same time there was an appreciable increase in the defect production.

One of the important advantages of MD simulation is that one can follow in complete detail the atomic trajectories and thereby obtain a picture of how the defect motion is occurring. In Fig. 1 we show a typical vacancy trajectory consisting of 15 jumps taken from a 16-psec ($\sim$120 vibrational periods) portion of the run at 1500 K. Only six of the ten (001) atomic planes and half of the atoms in each plane are drawn. The sequence of arrows indicates the vacancy-jump path. It is seen that a vacancy at site B preferentially jumped among the boundary sites rather than into the lattice. Since the nearest-neighbor distance in a bcc lattice is along the [111] directions, it is reasonable that vacancy jumps occurred more frequently from one (001) plane to another. Time sequences of local atomic configurations during vacancy jumps are shown in Fig. 2 for two different types of jumps. The projection of three (001) planes are drawn with the dotted, solid, and dashed circles representing the top, middle, and bottom layers, respectively. The diameter of the circle was taken to be $\frac{9}{10}$ of nearest-neighbor separation at the simulation temperature. During the simulation, the vacancy was observed to move continuously from one lattice site to another. In Fig. 2(a) an atom at site D in the top layer moved into the empty site B in the middle layer, the process occurring between 44×10^{-15} and 61×10^{-15} sec. The tracer plot originated from the center of the atom at D at $t=0$ shows that the jump trajectory of that atom is rather straight during the jump event which lasted about half a vibrational period. One can see that the neighboring atoms more or less maintained their positions so the surrounding configuration was quite rigid during the process. In Fig. 2(b) the sequence shows an atom at B' in the middle layer moving into an adjacent empty site B in the same layer. The tracer plot at $t=89\times10^{-15}$ sec reveals that the trajectory went through the interstitial site in the

TABLE I. Summary of various dynamic simulation runs.

T (K)	P (kbar)	N (time steps)	T (psec)	N (jumps)
900	1	5000	20	2
1100	1	10000	40	2
1300	4	117500	390	193
1400	3	117500	390	264
1500	3	117500	390	353
1600	3	57500	190	
1700	1	2500	10	
1800	13	27500	90	
1900	10	2500	10	
2100	100	1050	5	

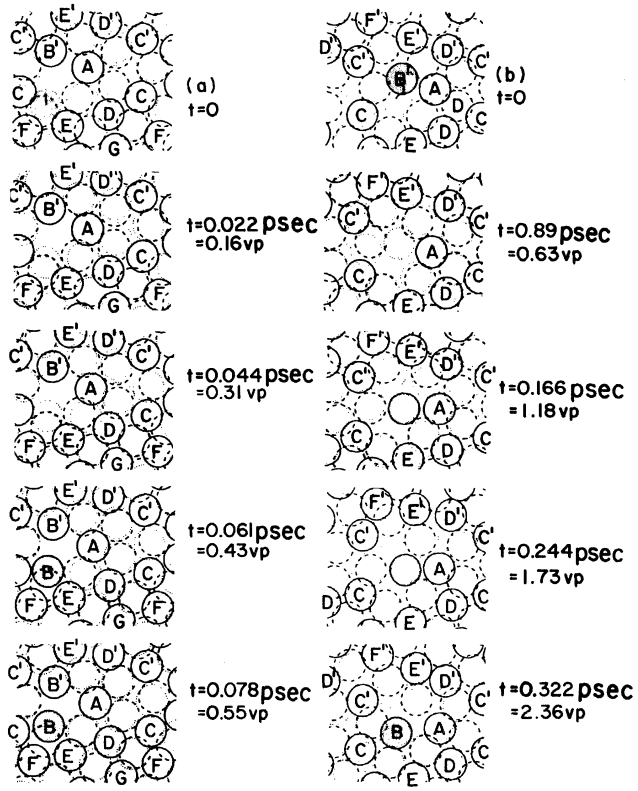

FIG. 2. Local atomic configurations projected onto (001) planes during a vacancy jump, atoms in the layer with the vacancy before the jump (solid circles) and those in the adjacent layers are indicated by dashed and dotted circles. The left sequence shows an atom at site D jumping into site B in the adjacent layer, while the right sequence shows a $B'\rightarrow B$ jump in the same layer. (vp denotes lattice vibrational period.)

layer above. This jump was completed in about two and a half vibrational periods. A rough estimate shows that the atoms typically traveled with thermal velocities.

At $T=1300$ K the GB structure remained stable and the vacancy readily identifiable over the entire period of simulation. This can be seen in Figs. 3 and 4. The projection of the atomic trajectories on each [001] plane is shown separately in Fig. 3. The initial atomic positions are denoted by circles with a diameter equal to $\frac{9}{10}$ of the nearest-neighbor distance. With the trajectory projected onto the layer to which the atom belonged initially, one does not see motions in the [001] direction in this representation. In Fig. 3 one sees that all the trajectories are essentially localized to the vicinity of initial atomic sites. Certain trajectories show movement to a position apparently at the center of a square structure (see, for example, the upper right region in the top layer); these correspond to nearest-neighbor jumps from one layer to an adjacent layer [cf. Fig. 2(b)]. It follows from this result that at $T=1300$ K there is essentially no translational disorder in the GB structure, and while the atomic jump is a discrete process from one site to another, the specific path followed can include an intermediate stop at an interstitial site. The dark region inside every circle indicates the amplitude of vibrational motion during the simulation. It is clear that vibrational amplitudes are, on the average, larger in the GB region than in the bulk lattice.

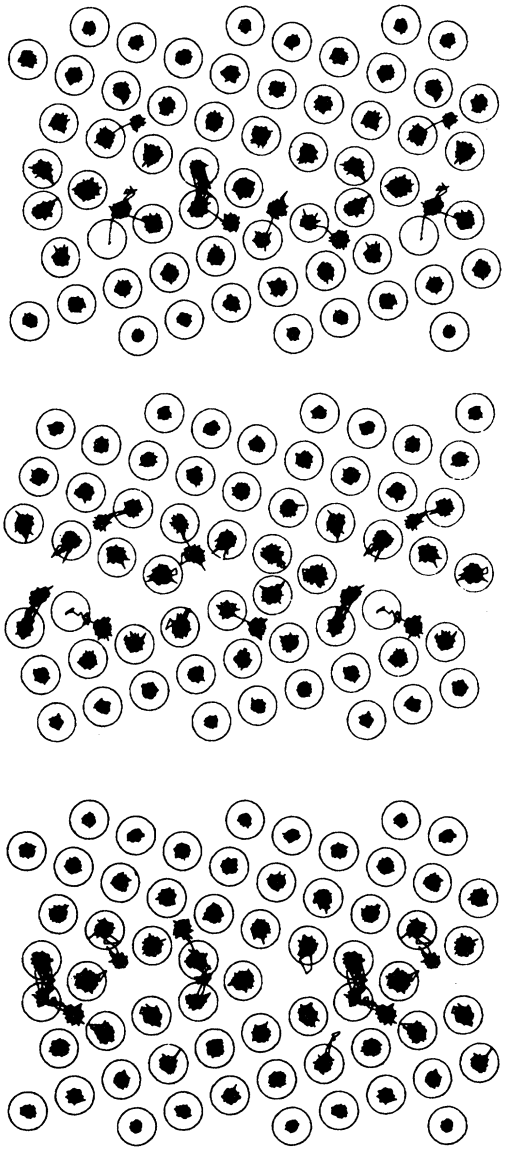

FIG. 3. Projected (001) plane view of trajectories in three adjacent layers accumulated over 0.39 nsec at $T=1300$ K. Vacancy started in the middle layer.

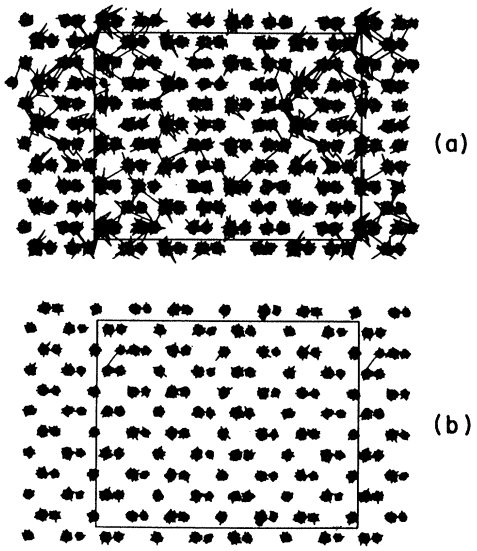

FIG. 4. Atomic trajectories showing motions projected on $(\bar{1}30)$ planes accumulated over 0.39 nsec at $T=1300$ K, (a) GB atoms at sites A, B, C, D; (b) bulk region atoms. Simulation cell is indicated by the box.

Figure 4 shows the trajectory projection on $(\bar{1}30)$ plane with the boundary region and the bulk shown separately. The motions in the [001], which is perpendicular to the tilt axis direction, are now indicated while those along $[\bar{1}30]$ are hidden. One sees a dramatic contrast in the extent of atomic motions. Many jumps from one layer to an adjacent layer occurred in the GB region while only one such jump took place in the bulk.

III. STRUCTURE DEPENDENCE

The discrete structure of the GB has a considerable influence on the vacancy-migration results observed in the present simulation. In a normal lattice, vacancies created in different lattice sites are all equivalent, so there is only one type of monovacancy jump. In the GB, vacancies in different boundary sites have different defect structures and formation energies (cf. paper I), so there are several distinct vacancy sites and thus different types of vacancy jumps.

An obvious indication of structure dependence is the variation in the number of vacancy jumps into different boundary sites. Results for the three temperatures are given in Table II, where we do not distinguish between equivalent primed and unprimed sites. Thus, at $T=1300$

TABLE II. Distribution of observed vacancy jumps into the various sites.

Sites	A	B	C	D	E	F	G	L	All
1300 K	3	126	20	32	7	6	1	0	195
1400 K	5	153	34	46	6	9	5	6	264
1500 K	9	197	49	62	11	18	3	4	353

K the 126 jumps into B sites include all jumps into B and B' among which will be jumps between B and B'. With increasing temperature, jumps which were previously confined to sites A, B, C, and D began to reach sites farther away from the boundary midplane, as one might expect for processes requiring thermal activation. In GB diffusion kinetics this signifies a transition from the so-called "Harrison type-C" regime to the "Harrison type-B" regime.[8] By comparing Table II with the vacancy binding energy for the various sites, one can observe a correlation indicating more frequent jumps into the sites with larger binding energy. Sites E, F, and G, being further from the core of the tilt boundary, received relatively few jumps, undoubtedly as a result of their smaller binding energies.

Another indication of structure dependence is the direction of jumps relative to the tilt axis. An anisotropic behavior is expected simply on the grounds that different local free volumes are available in the parallel and perpendicular directions. In the case of [001] tilt boundaries in Ag, diffusion was observed to be faster in the parallel direction.[9] The simulation data indeed show more jumps between adjacent [001] layers than jumps within a layer. A more detailed analysis reveals a difference in the migration direction after many jumps. If the system were perfectly symmetric in the sense of equal potential barriers for forward and backward jumps, then the only possibility

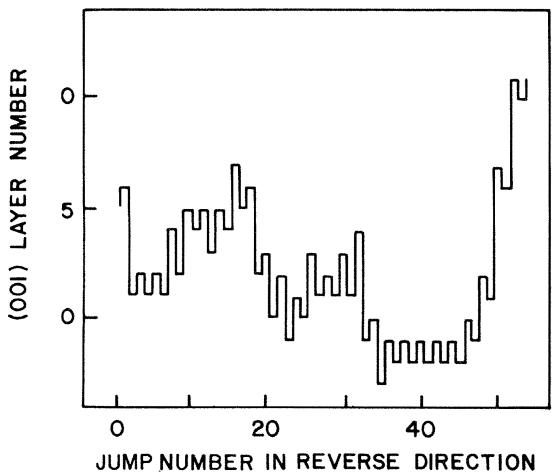

FIG. 5. Histogram of relative vacancy location, in units of (001) planes, showing persistence of jump direction with every reverse jump. Jumps within the same layer are not considered. Only the change between starting layer and final layer, so long as all the jumps are in the same direction, is shown without regard to time interval between jumps. Data obtained at $T=1300$ K.

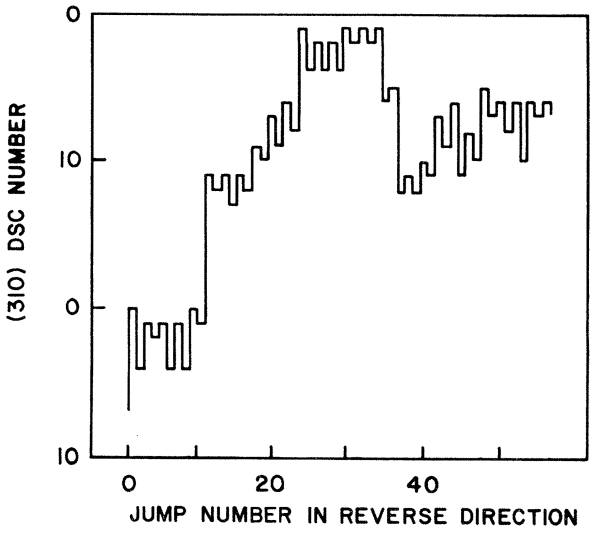

FIG. 6. Same as Fig. 5 except the jumps are along [310] in DSC (displacement shift complete) (Ref. 15) unit ($0.32a_0$), a direction perpendicular to the tilt axis.

for correlation between successive jumps would be a dynamical effect which is known to favor a second jump in the direction of the first jump. On the other hand, since there is no preference in the direction of the first move, by hypothesis, after many jumps one should find no net drift of the vacancy. We defer until the next section the question of short-time correlation effects, and consider now the evidence for overall isotropy along the parallel and perpendicular directions.

Figures 5 and 6 show the distribution of length of jump in a particular direction with reversal in jump direction without regard to the number of jumps and the time involved. One can see that over the total period of simulation there is effectively no net drift along the tilt axis, whereas a drift from right to left (cf. Fig. 1) is apparently taking place along the perpendicular direction [310]. Although the simulation period is long compared to time scales for dynamical correlation effects, we cannot be certain that the drift will not eventually reverse itself if the simulation were to continue. (In MD studies of GB sliding and migration, it was observed that once sliding was activated, it could continue quite a while before reversal set in. Here, too, it was not possible to demonstrate that sliding was equally possible in either direction.) On the other hand, the GB core does have an orientation, as indicated by the kite structure shown in Fig. 1, and we know that B-C jumps are more frequent than B-A jumps. Therefore, it is tempting to interpret our results as showing the effects of an inherent structural asymmetry.

IV. CORRELATION EFFECTS

In the discussion of correlation effects, one makes use of a reference model of vacancy motion as a random-walk process in which successive jumps are uncorrelated in time and direction. It is then expected that this model is valid only when the average time between jumps is much

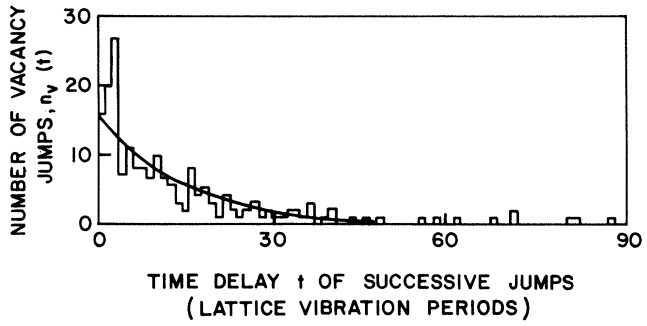

FIG. 7. Distribution of vacancy jumps as a function of time between successive jumps, $T=1300$ K.

longer than the relaxation time associated with the jump event. While there exists no simple operational definition of this relaxation time, it is relatively straightforward to study correlation effects given the trajectory data generated by MD.

The distribution of vacancy jumps at various times after a jump has occurred is shown in Fig. 7. Here, $n_v(t)$ is the probability of a second jump occurring between t and $t+\Delta t$ given that a jump has occurred at $t=0$. The curve in Fig. 7 denotes the exponential distribution which is appropriate to a random process,

$$n_v(t)=\frac{1}{\bar{t}}e^{-t/\bar{t}},$$

where the mean time between jumps $\bar{t}=T/N$ is determined in terms of the total simulation time T and the total number of vacancy jumps observed N. One sees that after a time of three vibrational periods the MD data show a significant enhancement over the random-walk distribution; this was found to be mainly due to the strong correlation between forward and reverse jumps involving close-packed atomic sites B and B'.[10] Otherwise, the data show essentially no correlation effects in time.

The distribution of second-jump directions relative to the first jump is shown in Table III along with the results expected for a random angular distribution. For a bcc lattice the occurrence of uncorrelated successive jumps would be in the ratio 1:3:3:1 for the indicated angular regions centered about $\cos\theta=-1$, -0.33, 0.33, 1, where θ is the angle between the two successive vacancy-jump directions. Thus, the fraction of reverse jumps expected is about $\frac{1}{8}$, in sharp contrast with the MD data.

TABLE III. Angular distribution of vacancy-jump direction relative to the previous jump at $T=1300$ K.

θ (deg)	$\cos\theta$	Actual	Random
0 to 35	1.00 to 0.82	0.104	0.125
35 to 90	0.82 to 0.00	0.307	0.375
90 to 145	0.00 to −0.82	0.115	0.375
145 to 180	−0.82 to −0.00	0.475	0.125

V. DIFFUSION KINETICS AND ATOMIC MEAN-SQUARE DISPLACEMENTS

The observation of many vacancy-jump events makes it possible to determine the activation energy for vacancy migration. If one assumes that vacancy exchange is the dominant mechanism for self-diffusion, then the present data can be used to estimate the self-diffusion coefficient.[7] In this section we will consider these two calculations along with a discussion of the mean-square displacements of atoms and vacancies.

A vacancy-jump frequency can be obtained by counting all types of jumps observed in the lifetime of a vacancy. When there exist several vacancy trajectories, an effective jump frequency $\tilde{\Gamma}$ can be defined by averaging the total numbers of jumps over the number of vacancy trajectories. An Arrhenius plot of $\tilde{\Gamma}$ is shown in Fig. 8 with error bars indicating the standard deviation estimated assuming a Poisson distribution. Fitting the data to

$$\tilde{\Gamma}=\tilde{\Gamma}_0\exp(-\tilde{E}_B^M/k_BT)$$

yields an effective activation energy (in eV) for GB vacancy migration,

$$E_B^M=0.51$$

and a preexponential factor $\tilde{\Gamma}_0=4.8\times10^{13}$ sec^{-1}. If we write for $\tilde{\Gamma}_0$,

$$\tilde{\Gamma}_0=\tilde{z}\tilde{\nu}_0\exp(\Delta\tilde{S}_V^M),$$

where $\tilde{z}$ is the effective coordination number, $\tilde{\nu}_0$ the effective "attempt frequency," and $\Delta\tilde{S}_V^M$ the effective entropy increase due to vacancy migration, then by taking $\tilde{z}=8$, $\Delta\tilde{S}_V^M=0$, we obtain a value of 6.1×10^{12} sec^{-1} for the effective attempt frequency. This may be compared with the vibrational frequency of 7.1×10^{12} sec^{-1} corresponding to a Debye temperature of 470 K for bcc iron.

The availability of vacancy-migration trajectories also suggests that it may be useful to view the sequence of jumps as a diffusion process characterized by a certain behavior of the mean-square displacement function $\langle\Delta^2r(n)\rangle$. Treating this problem as a random walk be-

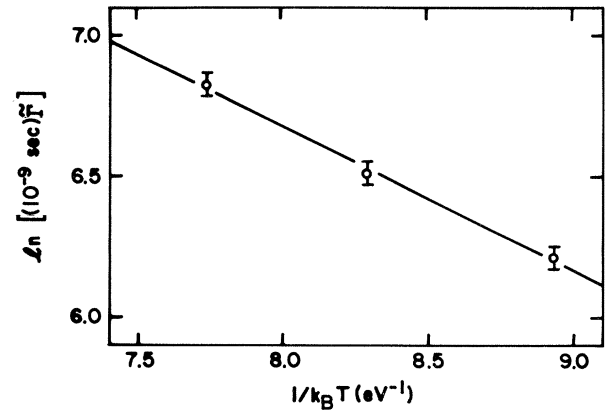

FIG. 8. Test of Arrhenius behavior of observed vacancy-jump frequency.

tween nearest-neighbor sites on a cubic lattice, one may write[11]

$$\langle \Delta^2 r(n) \rangle = n\alpha^2 \left[1 + \left\langle \frac{2}{n} \sum_{j=1}^{n-1} \sum_{i=1}^{n-j} \cos\theta_{i,i+j} \right\rangle_{\text{th}} \right] ,$$

where n is the number of steps, α the jump distance, and $\theta_{i,i+j}$, is the angle between the vacancy position $\vec{R}_i$, after i steps, and the position $\vec{R}_{i+j}$, after $i+j$ steps. $\langle\ \rangle_{\text{th}}$ indicates an average over various initial conditions consistent with a thermodynamic ensemble. If the vacancy jumps are strictly random, the second term in $\langle \Delta^2 r(n) \rangle$ vanishes and $\langle \Delta^2 r(n) \rangle = n\alpha^2$.

The square displacement of a vacancy in the case of a single vacancy trajectory is shown in Fig. 9. When many vacancy trajectories are obtained for different initial conditions, with a large number of jumps in each trajectory, a linear variation with time is expected of the averaged (mean-) square displacement. In this case it can be used to calculate the correlation factor which is a measure of the deviation from random walk[11]

$$f_v = \frac{\langle \Delta^2 r(n) \rangle_{\text{actual}}}{\langle \Delta^2 r(n) \rangle_{\text{random}}} .$$

For a crude estimate we fitted the vacancy trajectory shown to a straight line and obtained $f_v \sim 0.5$.

We next consider the atomic mean-square displacement (MSD) $\langle \Delta^2 r(t) \rangle$,

$$\langle \Delta^2 r(t) \rangle = \frac{1}{N} \sum_{i=1}^{N} [\vec{r}_i(t) - \vec{r}_i(0)]^2 .$$

In a diffusing system $\langle \Delta^2 r(t) \rangle$ behaves linearly with t at long times, so the self-diffusion coefficiently is then given by

$$D = \frac{1}{2s} \lim_{t \to \infty} \left[\frac{\langle \Delta^2 r(t) \rangle}{t} \right] ,$$

where $s = 3$ in the case of three dimensions.

In a perfect lattice the mean-square displacement will also show a linear growth with time so long as there is diffusion. However, this behavior occurs at times too long to be seen by MD simulation. What is expected is that $\langle \Delta^2 r(t) \rangle$ will increase to a bounded value which is proportional to the square of the atomic vibrational amplitude in the lattice. In a single lattice with a vacancy, diffusion occurs by the exchange of atoms with vacancy in a discrete manner. The mean-square displacement shows the same characteristics as that in a perfect lattice before the first atomic jump. Immediately after the jump event, the mean-square displacement would show a step increase, the step size being dependent on the jump distance and the number of atoms N involved in the averaging. Since vacancy jump is an infrequent event on the time scale of MD simulation, one should not expect the mean-square displacement to show a smooth linear variation with time, and this means an accurate determination of the diffusion coefficient would be difficult.

The MSD of all the atoms in the tilt boundary model at $T = 1100$ K over a short-time interval during which only two jumps have taken place is shown in Fig. 10. It shows the discrete behavior of a step increase with each atomic jump. Figure 11 shows the MSD of all the atoms in the same model at $T = 1300$ K now over a long time interval during which almost 200 jumps have taken place. (The distribution of bars under the curve indicates when a jump event occurs and what kind of jump event it is. The long bar corresponds to vacancy jumps among different sites. The medium bar corresponds to the forward and reverse jumps, while the short bars indicate those jumps involving the same pair of sites.) One can begin to discern a more or less linear behavior on a coarse-grained scale. By averaging over a number of such mean-displacement curves generated with different initial conditions one can hope to deduce a resonably accurate value of the self-diffusion coefficient. There remains the problem of deciding which atoms in the given boundary models should be considered in calculating $\langle \Delta^2 r(t) \rangle$. One solution would be to consider all the atoms to which the vacancy

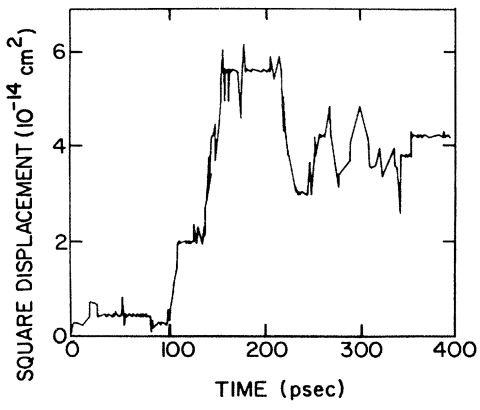

FIG. 9. Observed squared displacement of a vacancy in the GB core at $T = 1300$ K.

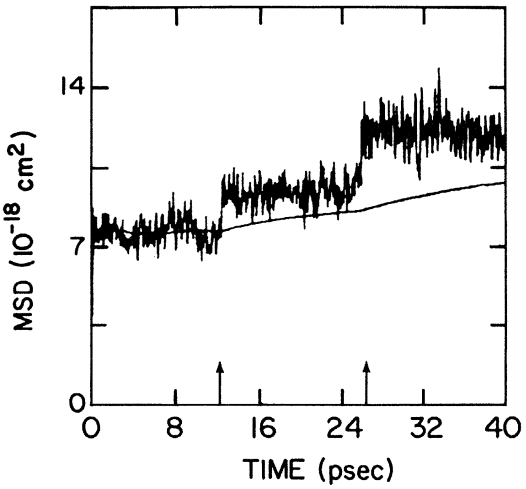

FIG. 10. Mean-square displacement of all the atoms in the GB model at $T = 1100$ K. Two jumps (indicated by arrows) have occurred during the time interval shown. Solid line denotes the cumulative average value.

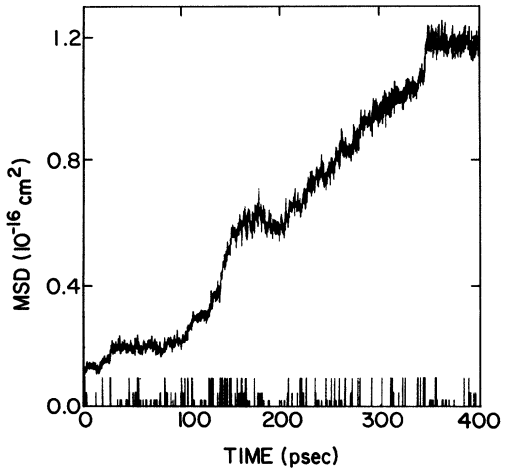

FIG. 11. Mean-square displacement of all the atoms in the GB model at $T=1300$ K. Note change of time scale from Fig. 10.

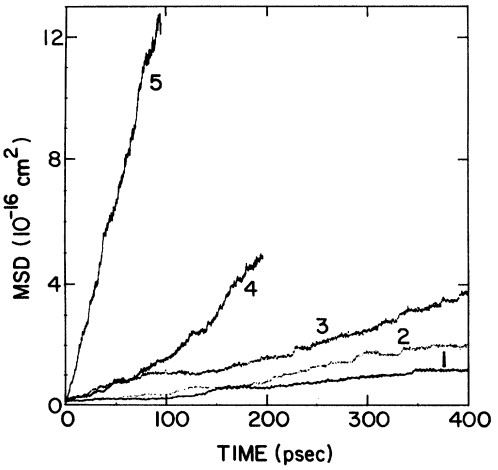

FIG. 13. Mean-square displacement of all the atoms in the GB model at various temperatures, (1) 1300, (2) 1400, (3) 1500, (4) 1600, and (5) 1800 K.

will jump and weigh the sites proportional to the frequency of vacancy jumps.

Figure 12 shows the mean-square displacement results obtained by averaging over atoms in the GB core (sites *A*, *B*, *C*, and *D*), atoms in the bulk (sites *E*, *F*, *G*, and *L*), and all the atoms in the simulation system. Since the GB thickness is now a well-defined quantity there is an intrinsic ambiguity in defining the GB diffusion coefficient. Figure 13 shows the behavior of $\langle \Delta^2 r(t) \rangle$ when all the atoms in the simulation system are taken into account.

We can make an estimate of the diffusion coefficient using the mean-square displacement information. The diffusion coefficient D^* for the simulation system is first obtained by fitting in the boundary sites (*A*, *B*, *C*, and *D*) at long time,

$$D^* = \frac{1}{6t} \langle \Delta^2 r(t) \rangle \ .$$

Then the self-diffusivity at equiibrium vacancy concentration can be calculated from

$$D = \exp(\Delta \tilde{S}_v^F) \exp\left[-\frac{\tilde{E}_B^F}{k_B T} \right] \frac{D^*}{N_V^*} \ ,$$

where $N_V^* = 0.25 \times 10^{-2}$ is the vacancy concentration for the simulation model. The self-diffusivity D calculated corresponds to a grain size of $6.5a_0$ and a boundary width $2.1a_0$. Using $\Delta \tilde{S}_V^F = 2$ and $\tilde{E}_B^F = 1$ eV, the Arrhenius plot of the grain-boundary diffusion coefficient is shown in Fig. 14. The melting point of the system is assumed to be close to the experimental value, $T_m = 1800$ K. The effect of including more atoms away from the boundary is to give an average diffusion coefficient for a thicker boundary region extended over the bulk region, thus decreasing the magnitude of D^*. Since the boundary thickness is

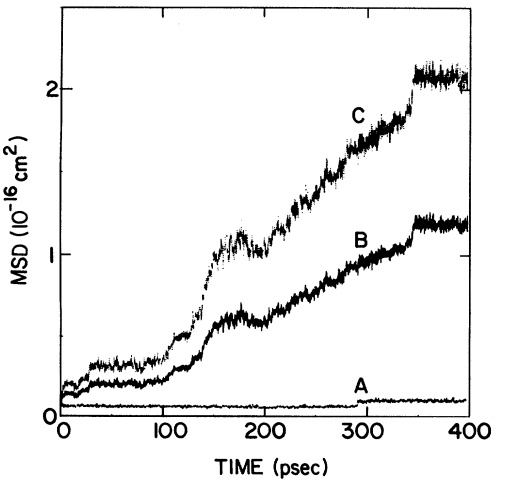

FIG. 12. Mean-square displacement of atoms in the GB (curve C) and bulk (curve A) regions at $T=1300$ K. Curve B, same as Fig. 11, is shown for comparison.

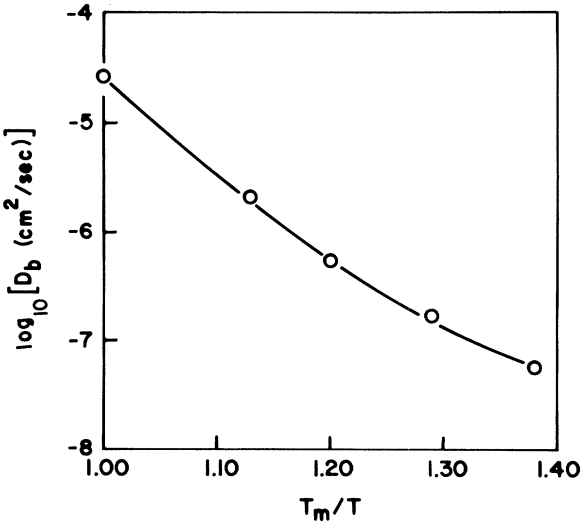

FIG. 14. Temperature variation of GB diffusion coefficients derived from the results of Fig. 13.

now well defined, it is often more useful to consider the product of D^* and boundary thickness.[2] Martin and Perraillon[12] have summarized the available GB diffusion data on the Arrhenius plot using a normalized reciprocal temperature scale. The D values given by Fig. 14 fall within the range of these experimental values.

VI. TRANSITION PROBABILITY FOR VACANCY JUMPS

We have observed the vacancy jumps to be strongly dependent on local structure. Since this is a general feature of vacancy migration, it would seem useful to characterize a particular GB structure by a corresponding transition probability matrix. The elements of such a matrix would then give the jump probabiities among the various discrete sites in the GB core. We define a matrix $|P|$, of which the elements P_{ij} are the probability that a vacancy will jump from site i to site j. P_{ij} can be decomposed as

$$P_{ij}=P_i p_{ij} ,$$

where P_i is the probability that site i is occupied by a vacancy, and p_{ij} is the conditional probability that, given a vacancy is localized at site i, it will next jump to site j. For normalization one clearly requires

$$\sum_i P_i=1$$

and

$$\sum_j p_{ij}=1 .$$

Then

$$\sum_i \sum_j P_{ij}=1 .$$

The matrix $|P|$ has been constructed using the vacancy-jump data at temperatures 1300, 1400, and 1500 K. Results for $T=1300$ K are given in Table IV. The dominant element is seen to be P_{BB} which actually refers to $B\rightarrow B'$ jumps. Notice that similar jumps between equivalent sites at other locations effectively did not occur because they involve much longer distances. In Table IV one can observe an asymmetry in that $P_{ij}\neq P_{ji}$; presumably this arises from the fact that sites i and j are at different levels of the potential energy surface so that one jump is "uphill" while the other is "downhill."

VII. DISCUSSION

In this work we have obtained MD results on vacancy migration and have related the data to self-diffusion. We believe our work demonstrates, first of all, the feasibility of studying the kinetics and structural properties of GB diffusion by means of computer simulation. The results illustrate the kind of information that one can extract from MD simulation data. While they are useful as general guides for further investigations, one should be careful in ascribing to them quantitative significance because of limitations due to inadequacies in the potential function and possible unphysical effects introduced by border conditions, finite system size, and insufficient statistical sampling. It is to be expected that some of the limiting factors will be dealt with in future work since they pertain to effects that can be controlled and systematically studied. Because of this and with the acquisition of more results on different GB structures, one can look forward to valuable insight to be gained from dynamical simulation studies.

It is worthwhile to stress again those aspects of the MD technique which make the simulation results useful. In essence, one is generating, through MD, detailed atomic trajectory data which are the numerical solutions to a sample of defect solid which obeys all the laws of classical mechanics and thermodynamics. The structural properties and kinetics are determined by interatomic forces evaluated using the instantaneous positions of the atoms; aside from border conditions there are no constraints on atomic displacements and hence deformations in the solid. In this respect, one has in the simulation all the nonlinearities inherent in relaxation and transport processes (at finite temperature and external stress), and the problem one faces is therefore not how to simulate such effects, but how to analyze and interpret the data to isolate a particular process of interest.

It is also worthwhile to comment on the need to go beyond the traditional view of diffusion in terms of vacancy exchange mechanism. This is quite clearly brought out in the present study. One difficulty with any mechanism involving point-defect exchange is that at elevated temperatures where large lattice deformations occur, a point defect can become delocalized, or no longer well defined because of significant increase of defect concentration. In our study the analysis of discrete vacancy jump became difficult at temperatures beyond 1600 K. Another difficulty is the evaluation of diffusion coefficient through jump frequency and correlation factor. The

TABLE IV. Elements of the transition probability matrix P_{ij} for vacancy jump from sites i to j at $T=1300$ K.

	A	*B*	*C*	*D*	*E*	*F*	*G*
A	0.0	0.005	0.010	0.0	0.0	0.0	0.0
B	0.0	0.485	0.052	0.108	0.0	0.0	0.0
C	0.015	0.072	0.0	0.010	0.005	0.0	0.0
D	0.0	0.082	0.031	0.0	0.026	0.026	0.0
E	0.0	0.0	0.010	0.021	0.0	0.0	0.005
F	0.0	0.0	0.0	0.026	0.005	0.0	0.0
G	0.0	0.0	0.0	0.0	0.0	0.005	0.0

latter is a quantity helpful in the physical interpretation of diffusion, but it is not easily extracted from the simulation.

One way to circumvent the difficulties of locating point defects and evaluating appropriate correlation factors is to describe diffusion entirely in terms of atomic coordinates which are always well defined and available from the simulation. One can adopt the definition of the diffusion coefficient D used in liquid state dynamics,

$$D=\frac{k_B T}{M}\int_0^\infty dt\,\psi(t)\ ,$$

where

$$\psi(t)=\langle \vec{v}(t)\cdot\vec{v}(0)\rangle/\langle \vec{v}(0)\cdot\vec{v}(0)\rangle$$

is the velocity autocorrelation function of an atom. It is not difficult to compute $\psi(t)$ by MD. Applying this approach to the GB diffusion problem requires *a priori* determination of which atoms can participate in the diffusion process.[13] This is equivalent to the specification of GB thickness. The advantage of the approach is that it is valid for any state of the system and makes use only of atomic trajectory rather than the trajectory of any defect.

In this work we have suggested the use of a transition probability matrix $|P|$ for vacancy jumps to represent, in operational terms, the structural characteristics of a GB system. The estimation of $|P|$ using MD is of interest for another reason. From the knowledge of $|P|$ one can carry out Monte Carlo simulation of vacancy migration and determine in this way the atomic mean-square displacement, the basic quantity in any discussion of diffusion. Although we have already examined $\langle \Delta^2 r(t)\rangle$ results in Sec. V, it would be very valuable to have data for more vacancy jumps than we can afford to accumulate using MD. By switching to a Monte Carlo simulation one can bypass the problem of waiting for a vacancy jump to occur and follow instead a migration path where every move of the system involves a vacancy jump.[14] To be sure, one loses short-time (and detailed) information concerning the jump process, but it is not altogether clear at this point that this information, beyond what is already built into $|P|$, is essential for the understanding of GB diffusion.

ACKNOWLDGMENTS

We would like to acknowledge the collaboration of P. D. Bristowe, R. W. Balluffi, and A. Brokman, especially during the early phase of the work. A portion of the work carried out at the Massachusetts Institute of Technology was supported by the Army Research Office.

[1]N. L. Peterson, Int. Metall. Rev. 28, 65 (1983).
[2]R. W. Balluffi, Metall. Trans. 13B, 527 (1982).
[3]G. Martin, D. A. Blackburn, and Y. Adda, Phys. Status Solidi 23, 223 (1967).
[4]J. T. Robinson and N. L. Peterson, Acta Metall. 21, 1181 (1973).
[5]T. Kwok, P. S. Ho, and S. Yip, preceding paper, this issue, Phys. Rev. B 29, 5354 (1984).
[6]A brief report of some of our results has been made in T. Kwok, P. S. Ho, S. Yip, R. W. Balluffi, P. D. Bristowe, and A. Brokman, Phys. Rev. Lett. 47, 1148 (1981) and also in Ref. 7.
[7]R. W. Balluffi, T. Kwok, P. D. Bristowe, A. Brokman, P. S. Ho, and S. Yip, Scr. Metall. 15, 951 (1981).
[8]L. G. Harrison, Trans. Faraday Soc. 57, 1191 (1961).
[9]R. E. Hoffman, Acta Metall. 4, 97 (1956).
[10]A. DaFano and G. Jacucci, Phys. Rev. Lett. 39, 950 (1977).
[11]J. R. Manning, *Diffusion Kinetics for Atoms in Crystals* (Van Nostrand, New York, 1968).
[12]G. Martin and B. Perraillon, in *Grain Boundary Structure and Kinetics,* edited by R. W. Balluffi, (American Society of Metals, Metals Park, Ohio, 1980), p. 239.
[13]The velocity autocorrelation function approach to grain-boundary diffusion has been recently discussed by G. Ciccotti, M. Guillope, and V. Pontikis, Phys. Rev. B 27, 5576 (1983).
[14]This method has been employed in the case of diffusion in fcc crystals, C. H. Bennett and B. J. Alder, J. Phys. Chem. Solids. 32, 2111 (1971).
[15]W. Bollman, *Crystal Defects and Crystalline Interfaces* (Springer, Berlin, 1970).